Microbiotyping the sinonasal microbiome

Ahmed Bassiouni[1], Sathish Paramasivan[1], Arron Shiffer[2], Matthew R Dillon[2], Emily K Cope[2], Clare Cooksley[1], Mahnaz Ramezanpour[1], Sophia Moraitis[1], Mohammad Javed Ali[3], Benjamin Bleier[4], Claudio Callejas[5], Marjolein E Cornet[6], Richard G Douglas[7], Daniel Dutra[8], Christos Georgalas[6], Richard J Harvey[9,10], Peter H Hwang[11], Amber U Luong[12], Rodney J Schlosser[13], Pongsakorn Tantilipikorn[14], Marc A Tewfik[15], Sarah Vreugde[1], Peter-John Wormald[1], J Gregory Caporaso[2], and Alkis J Psaltis[1]

[1] Department of Otolaryngology, Head and Neck Surgery, University of Adelaide, Adelaide, Australia

[2] Pathogen and Microbiome Institute, Northern Arizona University, Arizona, USA

[3] Dacryology Service, LV Prasad Institute, Hyderabad, India

[4] Department of Otolaryngology, Massachusetts Eye and Ear Infirmary, Harvard Medical School, Boston, USA

[5] Department of Otolaryngology, Pontificia Universidad Catolica de Chile, Santiago, Chile

[6] Department of Otorhinolaryngoloy, Amsterdam UMC, Amsterdam, The Netherlands

[7] Department of Surgery, University of Auckland, Auckland, New Zealand

[8] Department of Otorhinolaryngology, University of Sao Paulo, Sao Paulo, Brazil

[9] Department of Otolaryngology, Rhinology and Skull base, University of New South Wales, Sydney, Australia

[10] Faculty of Medicine and Health sciences, Macquarie University, Sydney, Australia

[11] Department of Otolaryngology -Head and Neck Surgery, Stanford University, Stanford, California, USA

[12] Department of Otolaryngology -Head and Neck Surgery, University of Texas, Texas, USA

[13] Department of Otolaryngology, Medical University of South Carolina, Charleston, South Carolina, USA

[14] Department of Otorhinolaryngology, Faculty of Medicine, Siriraj Hospital, Mahidol University, Bangkok, Thailand

[15] Department of Otolaryngology - Head and Neck Surgery, McGill University, Montreal, Canada

Corresponding author:

Associate Professor Alkis J Psaltis

3C (Department of Otolaryngology, Head and Neck Surgery)

The Queen Elizabeth Hospital

28 Woodville Rd

Woodville South, SA 5011

Australia

Email: alkis.psaltis@adelaide.edu.au

Phone: +61 08 8222 7158

Fax: +61 08 8222 7419

Funding information, Disclosures and Conflicts of Interest (COI):

Mohammad Javed Ali:

Receives royalties from Springer for his treatise "Principles and Practice of Lacrimal Surgery" and "Atlas of Lacrimal Drainage Disorders".

No conflict of interest relevant to this study.

Ahmed Bassiouni, Clare Cooksley, Mahnaz Ramezanpour, Sophia Moraitis:

No conflict of interest to declare.

Benjamin Bleier:

Grant Funding: R01 NS108968-01 NIH/NINDS (Bleier PI) – This isn't relevant to this study.

Consultant for: Gyrus ACMI Olympus, Canon, Karl Storz, Medtronic, and Sinopsys.

Equity: Cerebent, Inc, Arrinex.

COI: None relevant to this study.

Claudio Callejas:

No conflict of interest to declare.

J Gregory Caporaso, Matthew R Dillon, Arron Shiffer:

No conflicts of interest to declare. This work was funded in part by National Science Foundation Award 1565100 to JGC.

Emily K Cope:

Financial information: This work was partially funded under the State of Arizona Technology and Research Initiative Fund (TRIF), administered by the Arizona Board of Regents, through Northern Arizona University.

No relevant disclosures or COI.

Marjolein E Cornet:

No financial relationships or sponsors. No conflicts of interests.

Richard G Douglas:

Received consultancy fees from Lyra Therapeutics and is a consultant for Medtronic. These are not relevant to this study.

Daniel Dutra:

No conflict of interest to declare.

Richard J Harvey:

Consultant with Medtronic, Olympus and NeilMed pharmaceuticals. He has also been on the speakers' bureau for Glaxo-Smith-Kline, Seqiris and Astra-Zeneca.

No direct conflict of interest to declare.

Christos Georgalas:

No conflicts of interest to declare.

Peter H Hwang:

Financial Relationships: Consultancies with Arrinex, Bioinspire, Canon, Lyra Therapeutics, Medtronic, Tivic.

Conflicts of Interest: None.

Amber U Luong:

Serves as a consultant for Aerin Medical (Sunnyvale, CA), Arrinex (Redwood City, CA), Lyra Therapeutics (Watertown, MA), and Stryker (Kalamazoo, MI) and is on the advisory board for ENTvantage (Austin, TX).

Her department receives funding from Genetech/Roche (San Francisco, CA) and AstraZeneca (Cambridge, England).

No COI to declare related to this study.

Sathish Paramasivan:

Supported by a Garnett Passe and Rodney Williams Memorial Foundation Academic Surgeon Scientist Research Scholarship.

No conflicts of interest to declare.

Alkis J Psaltis:

Consultant for Aerin Devices and ENT technologies and is on the speakers' bureau for Smith and Nephew. Received consultancy fees from Lyra Therapeutics. These are not relevant to this study.

Rodney J Schlosser:

Grant support from OptiNose, Entellus, and IntersectENT (not relevant to this study). Consultant for Olympus, Meda, and Arrinex (not relevant to this study).

Pongsakorn Tantilipikorn:

No financial disclosures or conflict of interest.

Marc A Tewfik:

Principal Investigator: Sanofi, Roche/Genentech, AstraZeneca.

Speaker/Consultant: Stryker, Ondine Biomedical, Novartis, MEDA, Mylan.

Royalties for book sales: Thieme.

Sarah Vreugde:

No conflicts of interest relevant to this study.

Peter-John Wormald:

Receives royalties from Medtronic, Integra, and Scopis, and is a consultant for NeilMed. These are not relevant to this study.

Abstract

This study offers a novel description of the sinonasal microbiome, through an unsupervised machine learning approach combining dimensionality reduction and clustering. We apply our method to the International Sinonasal Microbiome Study (ISMS) dataset of 410 sinus swab samples. We propose three main sinonasal 'microbiotypes' or 'states': the first is *Corynebacterium*-dominated, the second is *Staphylococcus*-dominated, and the third dominated by the other core genera of the sinonasal microbiome (*Streptococcus*, *Haemophilus*, *Moraxella*, and *Pseudomonas*). The prevalence of the three microbiotypes studied did not differ between healthy and diseased sinuses, but differences in their distribution were evident based on geography. We also describe a potential reciprocal relationship between *Corynebacterium* species and *Staphylococcus aureus*, suggesting that a certain microbial equilibrium between various players is reached in the sinuses. We validate our approach by applying it to a separate 16S rRNA gene sequence dataset of 97 sinus swabs from a different patient cohort. Sinonasal microbiotyping may prove useful in reducing the complexity of describing sinonasal microbiota. It may drive future studies aimed at modeling microbial interactions in the sinuses and in doing so may facilitate the development of a tailored patient-specific approach to the treatment of sinus disease in the future.

Keywords

microbiome, sinus, next-generation sequencing, 16S rRNA gene, chronic rhinosinusitis, microbiotype

MAIN TEXT

Chronic rhinosinusitis (CRS) is a heterogenous, multi-factorial inflammatory disorder with a complex and incompletely understood aetiopathogenesis.[1] A potential role of the sinonasal microbiome and its "dysbiosis" in CRS pathophysiology has recently gained increased interest. The nature of the microbial dysbiosis and its role in disease causation and progression however remains unclear, with conflicting findings from the small sinonasal microbiome studies published thus far.

We recently reported the findings of our multi-national, multicenter "International Sinonasal Microbiome Study" or ISMS.[2] This study, the largest and most diverse of its kind to date, attempted to address many of the limitations of the smaller previous studies, by standardizing collection, processing and analysis of the samples. Furthermore, its large sample size and multinational recruitment, meant that it was more likely to capture geographical and centre-based differences if present. A recent meta-analysis of published sinonasal 16S rRNA sequences revealed that the largest proportion of variance was attributed to differences between studies,[3] highlighting a role for performing a large multi-centre study that employed a unified methodology.

Contrary to the findings of previous studies, our international cohort showed no significant differences in alpha or beta diversity between the three groups of patients analyzed: healthy control patients without CRS and the two phenotypes of CRS patients, those with polyps (CRSwNP) and those without (CRSsNP). The study however revealed a potential grouping of samples as demonstrated on beta diversity exploratory analysis.[2] Accordingly, we hypothesized that the bacteriology of the sinuses could be categorized into various clusters of similar compositions. We inquired whether these potential groups would aid in describing the sinonasal microbial composition of patients or associate with clinical features. Similar attempts performed on gut microbiota in healthy individuals were termed *enterotyping*.[4] The clinical relevance of gut enterotypes remain the topic of research, and sometimes controversy. A previous exploration of clusters of sinus microbiota in patients was performed by Cope et al.[5] in which the authors

143 reported four compositionally distinct sinonasal microbial community states; the largest group of patients
144 were dominated by a continuum of Staphylococcaceae and Corynebacteriaceae demonstrating a
145 reciprocal relationship.[5]

146 In this manuscript, we attempt "microbiotyping" to explain interpatient heterogeneity of the bacterial
147 communities in the paranasal sinuses, and are the first to describe "sinonasal microbiotypes" across the
148 first large, multi-centre cohort of individuals with and without CRS. We model our analysis on previous
149 attempts of enterotyping the gut microbiome. We then describe the composition of these microbiotypes,
150 explore potential clinical associations and validate microbiotyping on a separate sinus microbiome
151 dataset.

152

RESULTS

Basic characteristics of the study cohort and beta diversity plots

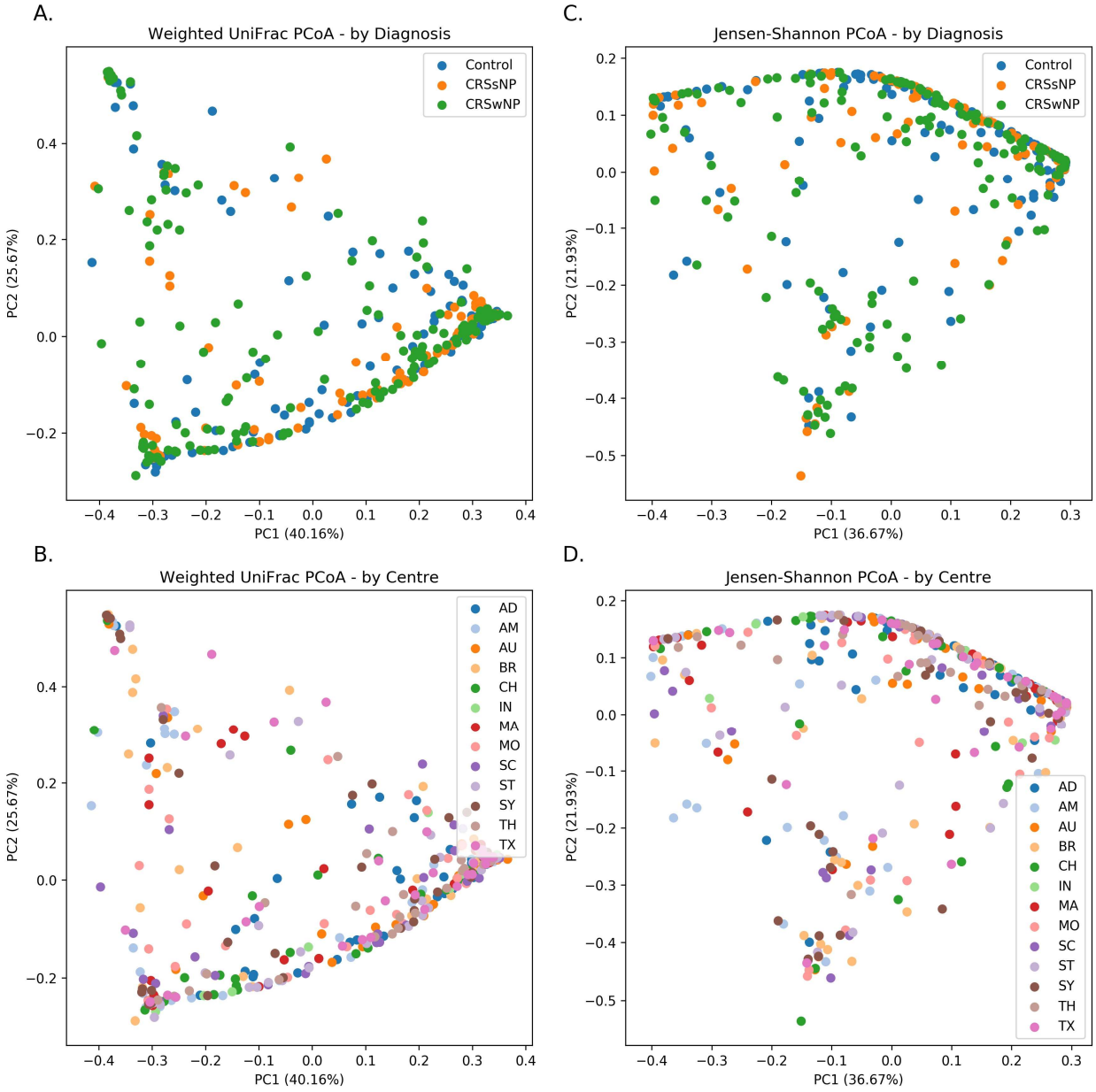

Figure 1: Beta diversity ordination plots.

The main ISMS study cohort was described in our previous publication.[2] In brief, 410 samples were included in the analysis collected from 13 centres representing 5 continents. These samples are distributed

along three diagnosis groups as follows: 99 CRSsNP patients, 172 CRSwNP patients, and 139 (non-CRS) controls. Beta diversity ordination plots (of weighted UniFrac and Jensen-Shannon distances) are shown in Figure 1. The plots do not reveal any distinct grouping by disease state or by centre, but on visual inspection show a triangular arrangement suggesting that samples lie on a continuum between three distinct clusters, providing motivation for further analysis.

Composition of the three sinonasal microbiotypes

We applied our microbiotyping approach through the unsupervised dimensionality reduction and clustering method described in the Methods. The composition of the resulting "sinonasal microbiotypes" is found in Figure 2A.

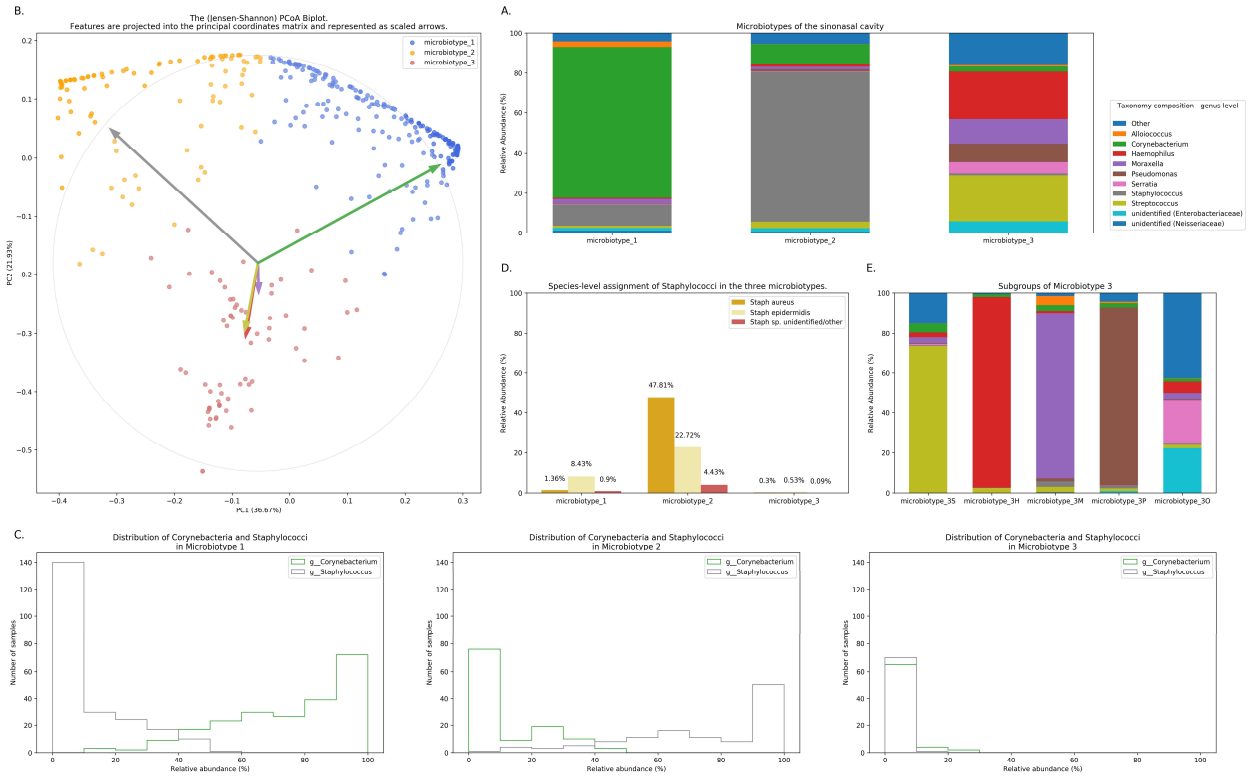

Figure 2: Microbiotyping the sinonasal microbiome. *(A) Taxonomic composition of the three microbiotypes at the genus level. (B) Illustration of the assigned microbiotypes on the Jensen-Shannon PCoA biplot. Arrows were used to depict the projection of the genera onto the PCoA matrix. Each arrow is indicated by the color of the genus according to the Legend. (C) Histograms demonstrating the relative*

173 *abundance of Corynebacterium and Staphylococcus. (D) Distribution of staphylococcal species (mean*
174 *relative abundance). (E) Subgroups of microbiotype 3 (hierarchical density-based clustering).*

175 Microbiotype 1 is dominated by *Corynebacterium* (mean relative abundance of 75.29%). Microbiotype 2
176 is dominated by *Staphylococcus* (mean relative abundance of 74.96%). Microbiotype 3 contained samples
177 that were mostly constituted of *Streptococcus*, *Haemophilus*, *Moraxella*, *Pseudomonas* and other genera.

178 The Abundance/Prevalence tables for the microbiotypes is demonstrated in Supplementary Tables S1A,
179 S1B and S1C.

180 We used a PCoA biplot to project features (genera) onto the PCoA matrix.[6] The 5 topmost abundant
181 genera were overlaid on the PCoA plot as arrows, originating from the centre of the plot and pointing to
182 the direction of the projected feature coordinates. (Figure 2B) Each arrow is indicated by the color of the
183 genus according to the Legend in Figure 2A, and the length of each was normalized as a percentage of the
184 longest arrow. The coloring of the samples in 2B in the PCoA scatter plot according to the microbiotype
185 assignment is provided for additional illustration. (Figure 2B) We note that the biplot arrows show a
186 quasi-orthogonal arrangement between the key genera that constitute the microbiome.

187 The distributions of the relative adundances of *Corynebacterium* and *Staphylococcus* in all three
188 microbiotypes were plotted in histograms (Figure 2C). It was noted that in microbiotype 1, most samples
189 have a high abundance of Corynebacteria (i.e. Corynebacteria dominate), while Staphylococci appeared
190 to dominate in microbiotype 2 in most samples.

191 **Dissection of "sinonasal microbiotype 3"**

192 We observed that Microbiotype 3 included various genera that did not cluster into the major two
193 microbiotypes. It was also evident that this microbiotype is more heterogeneous. Applying the K-Means
194 algorithm we showed poor clustering on only the first two and three Principal Components, since this
195 group included multiple signatures with various dominant organisms. Accordingly, we employed the

196 hieararchical density-based clustering algorithm "hdbscan"[7] on the full-dimensional OTU table. One
197 advantage of this algorithm is that it can estimate the number of clusters, without *a priori* specification by
198 the user. This algorithm also has the ability to detect "outliers" that fail to cluster with the rest of the
199 groups and detaches them into a separate "Miscellaneous/Other" group. We ran this algorithm on samples
200 in Microbiotype 3 and this revealed four clusters, each dominated by one of the genera of *Streptococcus*
201 (21 samples), *Haemophilus* (16 samples), *Moraxella* (9 samples), and *Pseudomonas* (7 samples), with a
202 mean relative abundance ranging from 73.49% to 95.5%. The fifth cluster was the assigned
203 "Miscellaneous/Other" group (18 samples). We term these "sub-microbiotypes": microbiotype 3S, 3H,
204 3M, 3P, and 3O, respectively. (Figure 2E)

205 **Exploring microbiotypes at the species-level reveals potential antagonism between**
206 **Corynebacterium species and Staphylococcus aureus**

207 At present, species level assignment is limited by the current technology of 16S-surveys, the current state
208 of microbial databases in general, and by our chosen short-read sequencing methodology. However,
209 species level associations hold clinical significance for sinus health, since *Staphylococcus aureus* has
210 been traditionally associated with biofilm formation and superantigen elaboration, both of which are
211 associated with more severe sinus disease and poorer response to treatment. Furthermore nasal carriage of
212 methicillin-resistant *Staphylococcus aureus* (MRSA) is a global health concern with implications that
213 extend far beyond the sinuses. Moreover, our new QIIME 2-based pipeline[8] allows a higher "sub-OTU"
214 resolution compared to older pipelines, offering an opportunity to resolve some taxa at species level when
215 possible.[9,10]

216 We explored taxonomy assignment at the species level, with a focus on Staphylococcal species.
217 Staphylococci were assigned to either *Staphyloccocus aureus*, *Staphylococcus epidermidis* or unclassified
218 *Staphylococcus*. We found that almost all of the assigned *Staphylococcus aureus* species were clustered in
219 Microbiotype 2, forming 47.81% mean relative abundance of this Microbiotype, compared to 1.36% and
220 0.3% in Microbiotype 1 and Microbiotype 3 respectively. (Figure 2E) Differential abundance of both

221 *Staphylococcus aureus* and *epidermidis* between the disease groups was confirmed as statistically
222 significant using ANCOM.

223 In light of this finding, we hypothesized a reciprocal or antagonistic relationship between
224 *Corynebacterium sp.* and *Staphylococcus aureus* and investigated this using SparCC. This confirmed a
225 significant negative correlation between Corynebacterium genus and the species *Staphylococcus aureus*
226 (SparCC correlation coefficient = -0.339, p = 0.001). Interestingly, *Staphylococcus epidermidis* positively
227 correlated with *Corynebacterium* (SparCC correlation coefficient = 0.271, p = 0.001). These results
228 should be interpreted cautiously in light of 16S-sequencing limitations. Nevertheless, they do appear to
229 correlate to previous findings in the literature, including *in vitro* experiments[11], a murine nasal bacterial
230 interaction model[12], and a survey of nasal vestibule swabs in healthy individuals[13]. These results suggest
231 that a benign or probiotic role is played by both *Corynebacterium spp.* and *Staphyloccocus epidermidis*
232 when interacting with *Staphylococcus aureus*.

233 **Prevalence and distribution of the microbiotypes in different diagnoses and centres**

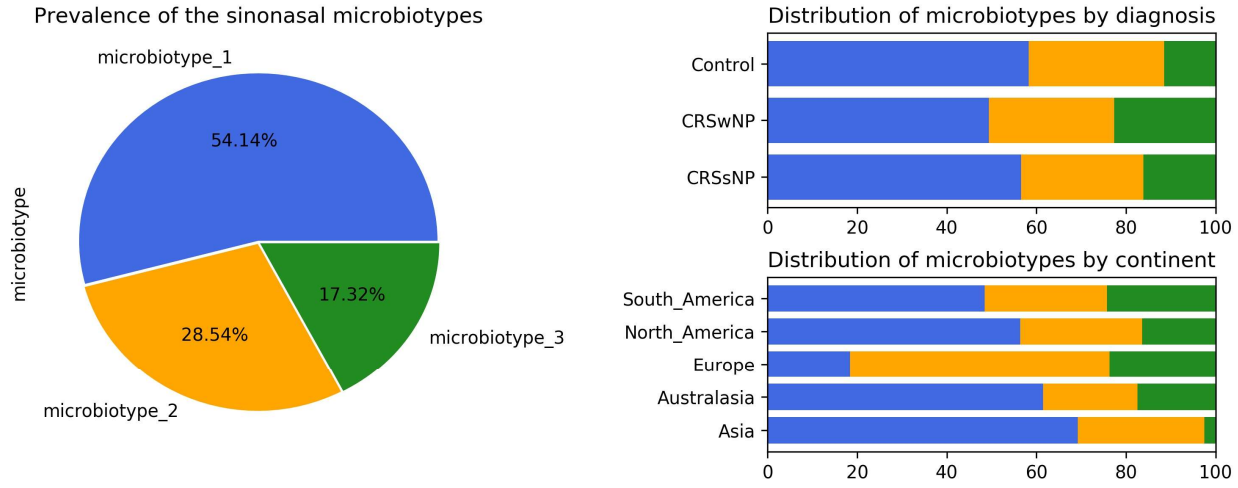

234

235 ***Figure 3: Prevalence and distribution of the microbiotypes.***

236 Microbiotype 1 was assigned to 222 samples (54.1%), microbiotype 2 to 117 samples (28.5%), and
237 microbiotype 3 to 71 samples (17.3%). The prevalence distribution of the sinonasal microbiotypes did not

238 appear to significantly differ by the disease state of the sinuses. (Figure 3) However, a Chi-Squared test
239 on the contingency table by centre showed significantly different distributions by centre (FDR-corrected p
240 < 0.001): there was a higher prevalence of microbiotype 2 in our European centre (Amsterdam), and a
241 higher prevalence of microbiotype 1 in Asian and Australasian centres, with a much lower prevalence of
242 microbiotype 3 in Asia. (Figure 3 and Table 1)

243 *Table 1: Distribution of microbiotypes by diagnosis and continent.*

variable	value	microbiotype_1	microbiotype_2	microbiotype_3	p value
Diagnosis	CRSsNP	56 (56.6%)	27 (27.3%)	16 (16.2%)	0.507
	CRSwNP	85 (49.4%)	48 (27.9%)	39 (22.7%)	
	Control	81 (58.3%)	42 (30.2%)	16 (11.5%)	
Continent	Asia	27 (69.2%)	11 (28.2%)	1 (2.6%)	< 0.001
	Australasia	67 (61.5%)	23 (21.1%)	19 (17.4%)	
	Europe	7 (18.4%)	22 (57.9%)	9 (23.7%)	
	North_America	89 (56.3%)	43 (27.2%)	26 (16.5%)	
	South_America	32 (48.5%)	18 (27.3%)	16 (24.2%)	

244

245 **Associations of microbiotypes with clinical variables**

246 We then explore the distribution of the three microbiotypes among multiple clinical variables in Table 2.
247 This shows no significant difference for some variables including asthma, aspirin sensitivity, GORD,
248 diabetes mellitus, and current smoking status, (FDR-corrected p > 0.05; Chi-squared test). The cross
249 tabulation however revealed a statistically significant association with “aspirin sensitivity” or aspirin-
250 exacerbated respiratory disease (AERD) (p = 0.02), although this did not persist after a Benjamini-
251 Hochberg correction (corrected p = 0.077). Patients who were aspirin-sensitive (or suffering from AERD)
252 showed less prevalence of microbiotypes 1, 2 and a higher prevalence of microbiotype 3, compared to
253 those who were not aspirin-sensitive. On the other hand, patients who were undergoing their “primary

surgery", had a higher prevalence of microbiotype 1 and a lower prevalence of microbiotype 3, compared to those patients who had had previous surgeries, but these results were not statistically significant.

Table 2: Distribution of microbiotypes by various clinical variables.

variable	value	microbiotype_1	microbiotype_2	microbiotype_3	p value
Asthma	No	162 (56.4%)	81 (28.2%)	44 (15.3%)	0.906
	Yes	55 (51.4%)	31 (29.0%)	21 (19.6%)	
Aspirin sensitivity	No	202 (55.3%)	106 (29.0%)	57 (15.6%)	0.077
	Yes	12 (48.0%)	5 (20.0%)	8 (32.0%)	
Diabetes	No	189 (54.9%)	98 (28.5%)	57 (16.6%)	0.979
	Yes	22 (55.0%)	11 (27.5%)	7 (17.5%)	
GORD	No	177 (55.3%)	93 (29.1%)	50 (15.6%)	0.979
	Yes	35 (55.6%)	17 (27.0%)	11 (17.5%)	
Current Smoker	No	204 (54.4%)	110 (29.3%)	61 (16.3%)	0.077
	Yes	15 (57.7%)	4 (15.4%)	7 (26.9%)	
Primary surgery	No	92 (47.2%)	57 (29.2%)	46 (23.6%)	0.114
	Yes	130 (60.5%)	60 (27.9%)	25 (11.6%)	

Validation of sinonasal microbiotyping on a separate dataset

We validated our approach on a separate 16S dataset we called Dataset Two. As described in the Methods section, we validated this using an independent unsupervised approach and a semi-supervised approach guided by the Main Dataset.

The first unsupervised approach yielded three clusters similar to the microbiotypes described on the Main Dataset, with one cluster exhibiting high mean relative abundance of Corynebacteria, a second cluster exhibiting high mean relative abundance of Staphylococcus, and a third cluster with other dominant genera. Plotting the first two Principal Components (Figure 4A) resulting from PCoA on the JSD matrix revealed the same triangular distribution of samples observed in Figure 1.

Prevalence of the microbiotypes in this dataset (using the unsupervised approach) was as follows: microbiotype 1 assigned 39.2% of samples, microbiotype 2 with 26.8% of samples, and microbiotype 3 with 34.0%.

The second semi-supervised approach yielded similar results (Figure 4; Supplementary Table), differing in the classification of only 3 samples (out of 97 samples; i.e. 3.09%). (See Supplementary Jupyter notebook) Two of these samples show *Staphylococcus* dominating the samples in combination with *Haemophilus*, with no overt dominance of one taxon over the other, making them more-or-less transitional samples between the signatures of microbiotypes 2 and 3. The third sample was dominated by *Staphyloccocus* and *Corynebacterium*, making it a transitional sample between microbiotype 1 and microbiotype 2, with Staphylococcal species assigned to *epidermidis*, making this more appropriately assigned to microbiotype 1. (see Supplementary Jupyter notebook)

These results validate the microbiotyping approach and suggest that our approach and dataset could be used to guide classification of sinonasal samples sequenced in future separate studies. (Figure 4) Moreover, it points towards a potential clinical relevance of performing sinonasal microbiotyping.

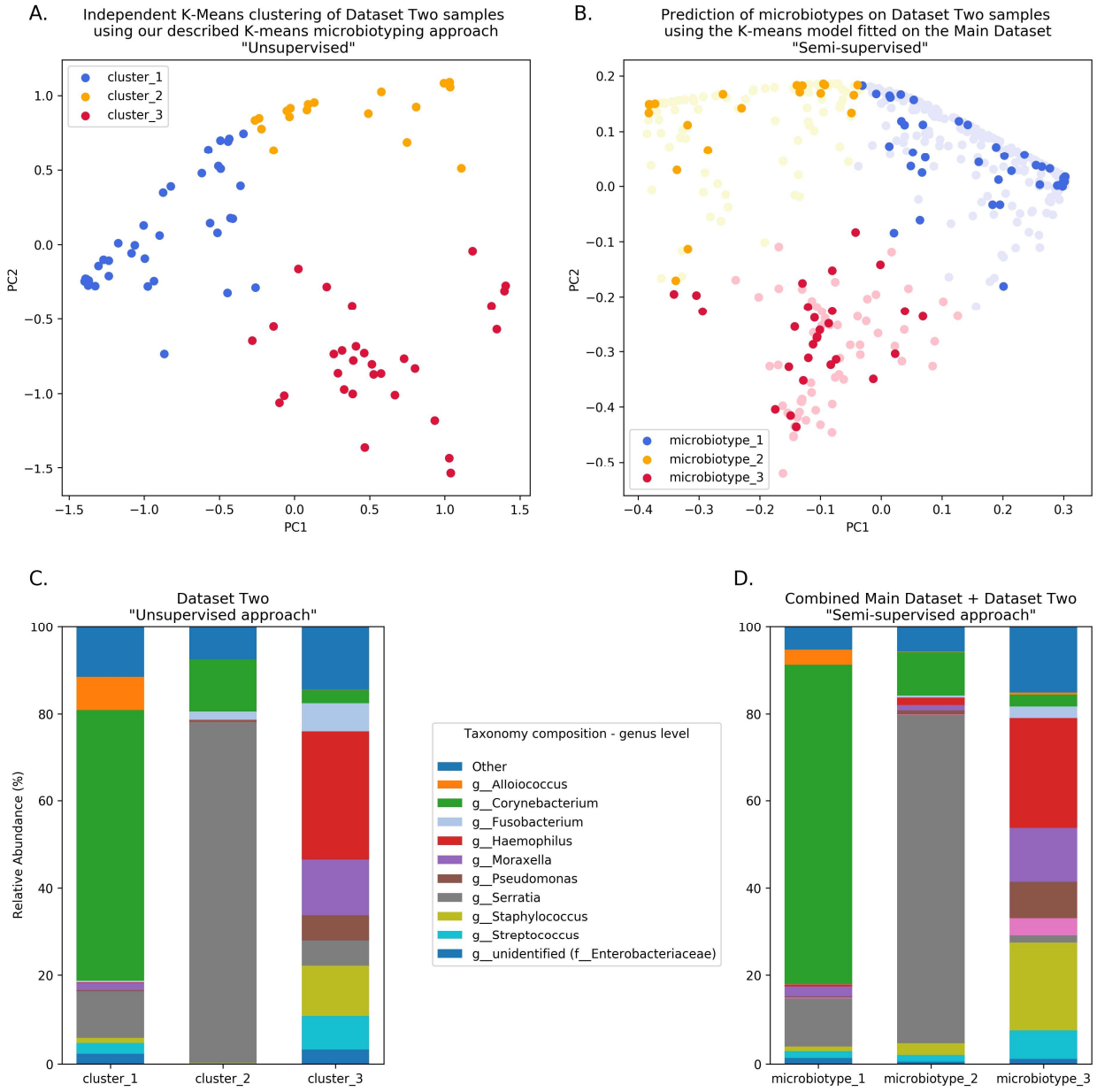

Figure 4: Validation of microbiotyping approach on Dataset Two.

DISCUSSION

We demonstrate that the microbiota of most sinus swab samples could be classified into distinct signatures or archetypes, which we have termed "sinonasal microbiotypes". We observed three main microbiotypes: the most prevalent being a *Corynebacterium*-dominated microbiotype (microbiotype 1), then a *Staphylococcus*-dominated microbiotype (microbiotype 2), and microbiotype 3 which includes samples dominated by *Streptococcus*, *Haemophilus*, *Moraxella*, *Pseudomonas*, and other genera (3S, 3H, 3M, 3P, and 3O respectively).

As we have previously reported,[2] the sinus microbiota are dominated by the genera *Corynebacterium* and *Staphylococcus* (microbiotypes 1 and 2). A similar clustering approach to the sinus microbiome was applied by Cope and colleagues, who utilized Dirichlet multinomial mixture models (DMMs),[5] and reported that most samples in their study were occupied by a continuum of Staphylococcaceae and Corynebacteriaceae.[5] It appears that, regardless the statistical or clustering methodology utilized, it is most likely that the sinonasal microbiome consists of core organisms[2] that have a distinct co-occurrence pattern. This could be explored through a network analysis approach and should be a future area of study.

Staphylococcus aureus has been perceived to be an important pathogen in sinus inflammatory disease. *Staphylococcus aureus* biofilms may act as a nidus for recurrent infections[14,15] and as a "nemesis" of otherwise-successful sinus surgery.[16–18] *Staphylococcus aureus* is also a producer of exotoxins, which in some cases can serve as superantigens, and these have been previously described as playing an important role in the pathogenesis of CRSwNP.[19] *Pseudomonas aeruginosa* biofilms are also virulent organisms that are difficult to eradicate from the sinuses, and have been associated with worse clinical outcomes.[20] Both these organisms are important pathogens in the chronic mucociliary dysfunction exhibited in cystic fibrosis. However, methicillin-resistant *Staphylococcus aureus* (MRSA) is an important nasal colonizer that could asymptomatically colonize the nose. What determines the clinical course, between asymptomatic colonization versus symptomatic pathogenicity, remains an interesting topic of research. In

308 this study, we identified a potential reciprocal relationship between *Staphylococcus aureus* and
309 *Corynebacterium*. Being aware of the challenges of compositional data analysis, we utilized for this
310 purpose the specialized SparCC algorithm which infers correlations from compositional data.[21] This
311 finding needs to be supported by future co-culture experiments, but suggests that *Corynebacterium sp.*
312 may be a "cornerstone" of sinus microbial health. It is important to note that our bioinformatic
313 methodology has been intentionally designed to utilize state-of-the-art software methods at every step of
314 the analysis pipeline, in order to maximise the resolution of taxonomy assignment.[8,9,22] Nevertheless, our
315 approach is still confined within the limitations of current 16S sequencing methodologies, and the
316 confidence of assignment is reduced beyond the genus level. Our analysis pipeline could not delineate
317 between different Corynebacterium at the species level and Staphylococcus aureus at the strain level.
318 Hence functional difference between samples with same species remain to be determined using a
319 functional metagenomics approach. A recent study suggest that by incorporating location information or
320 "sample-level metadata" into species-level assignment accuracy could be improved.[23] In our study, the
321 differential relationships of both *Staphylococcus aureus* and *epidermidis* towards *Corynebacteria*
322 (negative and positive associations, respectively) could be of clinical significance and is worthy of future
323 investigation. We performed a post-hoc inspection of species-level assignment in Dataset Two, to
324 investigate whether this finding will be reproducible in a separate dataset. This confirmed clustering of
325 almost all *Staphylococcus aureus* species in microbiotype 2. (Supplementary Results in Jupyter
326 Notebook)

327 Interestingly, we found that the distribution of the sinonasal microbiotypes was not significantly dis-
328 similar amongst healthy controls and CRS patients. There appeared to be no significant associations with
329 other clinical variables such as asthma and aspirin-sensitivity after controlling for multiple comparisons.
330 (Table 2) The distribution of the microbiotypes however differed according to centre/location of
331 collection. (Figure 3) As such, we cannot conclude based on our study that microbiotypes could function
332 independently as a disease biomarker. Although not reaching statistical significance (chi squared p >

333 0.05) the prevalence of microbiotype 3 was higher in CRSsNP and CRSwNP, compared to controls. It
334 could be the case that chronicity of inflammation -on its own- is not a determinant of a dysbiotic
335 microbiome, but whether there is a clinically-evident "sinus infection" current at the time of sample
336 collection. In this theory, stable chronic sinuses with no overt signs of acute or chronic infection, may
337 remain similar to a "healthy sinus microbiome". Only when the sinuses are clinically infected (as evident
338 on clinical symptoms and endoscopic findings), the microbiota become disrupted and the dysbiosis
339 exaggerated. It is important to note that *Streptococcus*, *Haemophilus* and *Moraxella* (represented here in
340 microbiotype 3) have been traditionally implicated in acute infections of the upper respiratory tract
341 including acute rhinosinusitis and acute otitis media. Unfortunately, information regarding acute
342 exacerbations was not explored within this study.

343 Regarding geographical differences: Asia and Australasia showed an over-representation of microbiotype
344 1. Europe had a higher prevalence of microbiotype 2. Unfortunately, the study only included one
345 European centre (Amsterdam) so it is difficult to be certain whether this finding generalizes to other
346 locations in Europe. The driving factors for these geographical differences could be multiple, including
347 but not limited to clinical practices such as local antibiotic prescriptions for CRS and timing of
348 recruitment of patients for sinus surgery, as discussed previously.[2]

349 We have adapted our methodology from the enterotyping approach taken by Arumugam et al.[4] for
350 classifying bacterial signatures of the gut microbiome. In their original manuscript, they described three
351 different enterotypes in the gut dominated by *Prevotella*, *Bacteroidetes*, and *Ruminococcus* respectively.[4]
352 Several papers have correlated gut enterotypes with various clinical variables.[24,25] Despite this,
353 enterotyping as an approach to population stratification has not been without its controversies. Several
354 authors have criticized the definition of distinct clusters, since it neglects intra-cluster variation and
355 gradients between clusters.[26–29] We provide answers to previous critique[28] to enterotyping as it applies to
356 our study in Supplementary Table S2. It is important to note these valid criticisms to any community
357 typing approach. In our experiment, the clusters or types lie on a continuum, with some samples falling in

358 the gradients between two, or perhaps even all three microbiotypes (see ordination plots). The histograms
359 in Figure 2 also suggest this, but they do show most samples in each microbiotype feature a high relative
360 abundance of a dominating genus in many samples. We investigated a simple dominance measure, the
361 Berger-Parker (BP) alpha diversity index,[30] in the combined datasets' 507 samples. The Berger-Parker
362 index simply reports the relative abundance of the most dominant taxon in a sample. This found that only
363 24.9% of samples had a dominating taxon that only had a relative abundance of 50% or less. On the other
364 hand, 51.9% of samples had the dominant taxon exhibiting a relative abundance of greater than 70% of
365 the sample.(Supplementary Results in Jupyter notebook; Supplementary Figure S1) This shows that in
366 most samples, there is one dominating organism. Based on these results, the microbiotyping approach is
367 therefore proposed to reduce complexity about modeling bacterial interactions in the sinuses, and not to
368 suggest that each type is a walled-off discrete cluster. Further investigations into the local substructures of
369 each type will be required to further explore the roles and interactions of its constituent taxa. Another
370 limitation of our description of microbiotypes is that they may as well describe different community
371 "states" rather than community "types", since we do not have longitudinal data to describe how these
372 clusters behave with the passage of time and treatments. Hence, we could not confirm whether these are
373 stable, consistent communities across time. It may well be that intermediate samples lying between two or
374 more microbiotypes are representing a transitional state. An important future avenue of research is to
375 conduct a longitudinal study to investigate the temporal stability of these clusters.

376 We predict that ongoing sinonasal microbiome research and consequent large meta-analyses of
377 microbiota studies, with novels tools (such as QIITA[31]) enabling such large-scale studies, will allow the
378 refinement of these types and further clarify their clinical/microbiological utility. Our methodological
379 approach to describe the microbiotypes is not exclusive, as alternative statistical or machine-learning
380 approaches could be employed to investigate them. In light of this, we expect that international multi-
381 centre standardization and rationalization of the sinonasal microbiotypes would be possible in the future,
382 similar to the recent proposed effort to standardize enterotyping of the gut microbiota by Costea et al.[29]

383 # CONCLUSION

384 We investigated the ISMS dataset through an approach modeled on human gut microbiome enterotyping
385 and we found three major microbial community types or "microbiotypes" as clusters that lie on a
386 continuum, based on an unsupervised machine learning approach that involved dimensionality reduction
387 and clustering. Microbiotypes did not show an association with disease state or clinical variable,
388 suggesting that they could not function as independent disease biomarkers. The description of these
389 microbiotypes has also unveiled a potential reciprocal relationship between *Staphyloccocus aureus* and
390 *Corynebacterium spp.* in the sinuses that requires further investigation in future studies. The findings
391 were validated on a separate previously unpublished sinus bacterial 16S gene dataset. Microbiotypes are
392 therefore proposed to reduce the complexity of modeling bacterial interactions in the sinuses, and in this
393 sense hold microbiological and clinical relevance that could potentially influence medical and surgical
394 treatment of CRS patients.

395

METHODS

The "International Sinonasal Microbiome Study (ISMS)" dataset

We perform the primary analysis on the dataset obtained from the "International Sinonasal Microbiome Study (ISMS)" project.[2] In summary, this dataset is a multi-centre 16S-amplicon dataset which includes endoscopically-guided, guarded swabs collected from the sinuses (in particular the middle meatus / anterior ethmoid region) of 532 participants in 13 centres representing 5 continents. Details of sample collection, DNA extraction and sequencing methodologies are described in the original report.[2] The 16S gene region sequenced was the V3–V4 hypervariable region, utilizing primers (CCTAYGGGRBGCASCAG forward primer) and (GGACTACNNGGGTATCTAAT reverse primer) according to protocols at the sequencing facility (the Australian Genome Research Facility; AGRF). Sequencing was done on the Illumina MiSeq platform (Illumina Inc., San Diego, CA) with 300-base-pairs paired-end Illumina chemistry

Bioinformatics pipeline

Details of the bioinformatic pipeline is detailed in the original report.[2] In summary, we utilized a QIIME 2-based pipeline.[8] Forward and reverse fastq reads were joined[32], quality-filtered,[33], abundance-filtered[34], then denoised using deblur[9] through QIIME 2-based plugins. This yielded a final feature table of high-quality, high-resolution Amplicon Sequence Variants (ASVs). Taxonomy assignment and phylogenetic tree generation[35] was done against the Greengenes[36] database; and taxonomy was assigned using the QIIME 2 BLAST assigner.[22] A rarefaction minimum depth cut-off was chosen at 400 and this yielded 410 samples out of the original 532 for downstream analysis. The same pipeline was then applied on DataSet Two for purposes of validation of microbiotyping. We chose to reproduce exactly all the original pipeline steps on DataSet Two, despite being a completely separate dataset, to reduce bias.

418 **Delineating the microbiotypes of the sinonasal microbiome**

419 Our approach was guided by the "enterotyping" method described by Arumugam et al.[4] with adaptations.
420 We constructed a sample distance matrix using the Jensen-Shannon distance (JSD) metric, as used in the
421 original "enterotypes" paper.[4] The Jensen-Shannon distances were calculated between samples in the
422 genus-level-assigned table in a pairwise fashion using the JSD function in the R package "philentropy"
423 with a log ($\log_{10}$) base. Following this, Principal Coordinate analysis (PCoA) was done on the distance
424 matrix for dimensionality reduction and visualization. Clustering was then performed using a standard K-
425 means clustering algorithm, as implemented in the machine learning Python package scikit-learn (version
426 0.20.1);[37]) on the first two principal components (PCs) obtained from the PCoA, with the number of
427 clusters (k) chosen at 3 based on visual inspection of the beta diversity PCoA plots. Average silhouette
428 scores, as implemented in scikit-learn, for the range (k = 2 - 8) were calculated to assess clustering
429 quality, and this revealed the highest silhouette scores: 0.61 and 0.6 for [k=4] and [k=3] respectively. The
430 three resulting clusters were defined as the three sinonasal microbiotypes. For further exploration of the
431 subgroups that constitute microbiotype 3, we used the hierarchical density-based clustering algorithm
432 "hdbscan"[7] on the full-dimensional feature table. Genera were projected onto the PCoA matrix using a
433 biplot approach[6], as implemented in scikit-bio's function *"pcoa_biplot"*. Genera were represented in the
434 biplot figure as arrows, originating from the centre of the plot pointing to the direction of the projected
435 feature coordinates, and the lengths normalized as a percentage of the longest arrow. We utilized
436 "Analysis of Compositions of Microbiomes (ANCOM)"[38] for identifying differentially-abundant taxa.
437 Taxa genus level and Staphylococcus species level co-occurrence/correlation analysis were done after
438 taxonomy assignment using SparCC algorithm,[21] in the fast implementation in FastSpar.[39]

439 **Validating microbiotypes on a second sinonasal microbiome dataset**

440 To infer whether our classification could be generalizable to other sinonasal microbiome samples not
441 included in this study, we sought to validate our microbiotyping approach on a separate, previously-
442 unpublished, 16S dataset. This dataset includes sinonasal microbiome swabs collected from private and

443 public patients attending the Otolaryngology Department (University of Adelaide) to have surgery done
444 by the authors P.J.W., A.J.P. or the Otorhinolaryngology Service at the Queen Elizabeth Hospital in
445 Adelaide, South Australia. Similar to the main dataset, these included CRS patients who underwent
446 endoscopic sinus surgery for this sinus disease, and non-CRS control patients who underwent other
447 otolaryngological procedures, such as tonsillectomy, septoplasty or skullbase tumour resection. Sample
448 collection, and processing were done in a standardized fashion similar to that has been described in the
449 ISMS main dataset, except that DNA extraction was carried out using the PowerLyzer Power-Soil DNA
450 kit (MoBio Laboratories, Salona Beach, CA) as previously described[40], rather than the Qiagen DNeasy kit
451 (Qiagen, Hilden, Germany). Similar to the ISMS samples, library preparation and 16S sequencing were
452 done at the Australian Genome Research Facility (AGRF) on the Illumina MiSeq platform (Illumina Inc.,
453 San Diego, CA, USA) with the 300-base-pairs paired-end chemistry. Libraries were generated by
454 amplifying (341F–806R) primers against the V3–V4 hypervariable region of the 16S gene
455 (CCTAYGGGRBGCASCAG forward primer; GGACTACNNGGGTATCTAAT reverse primer).[41] PCR
456 was done using AmpliTaq Gold 360 master mix (Life Technologies, Mulgrave, Australia) following a
457 two-stage PCR protocol (29 cycles for the first stage; and 8 cycles for the second, indexing stage).
458 Sequencing was done over two MiSeq runs in January 2015. We termed this dataset in this manuscript
459 "Dataset Two". This dataset comprises samples collected from 129 participants. Rarefaction at a cutoff of
460 400 reads was performed, to match what was performed for the main dataset, and samples with read
461 number less than 400 were excluded; this yielded a final feature table containing 97 samples, representing
462 33 CRSsNP patients, 35 CRSwNP patients, and 29 controls.

463 We took two separate approaches to validation. The first approach is to replicate the previously-described
464 unsupervised K-means microbiotyping methodology independently on samples in Dataset Two. We call
465 this first approach the "unsupervised approach". The second approach is to use the K-means model that
466 was fitted on the samples from the Main Dataset to predict labels (i.e. microbiotypes) of the samples in

Dataset Two. As such, the Main Dataset is used as a "training dataset" in the language of machine learning. We called the second approach the "semi-supervised approach".

Statistical Analysis

All frontend analyses were done using the Jupyter notebook frontend[42] and utilizing the assistance of packages from the Scientific Python[43] stack (numpy, scipy, pandas, statsmodels), scikit-learn[37], scikit-bio (https://github.com/biocore/scikit-bio) and omicexperiment (https://www.github.com/bassio/omicexperiment).

Supplementary Figures

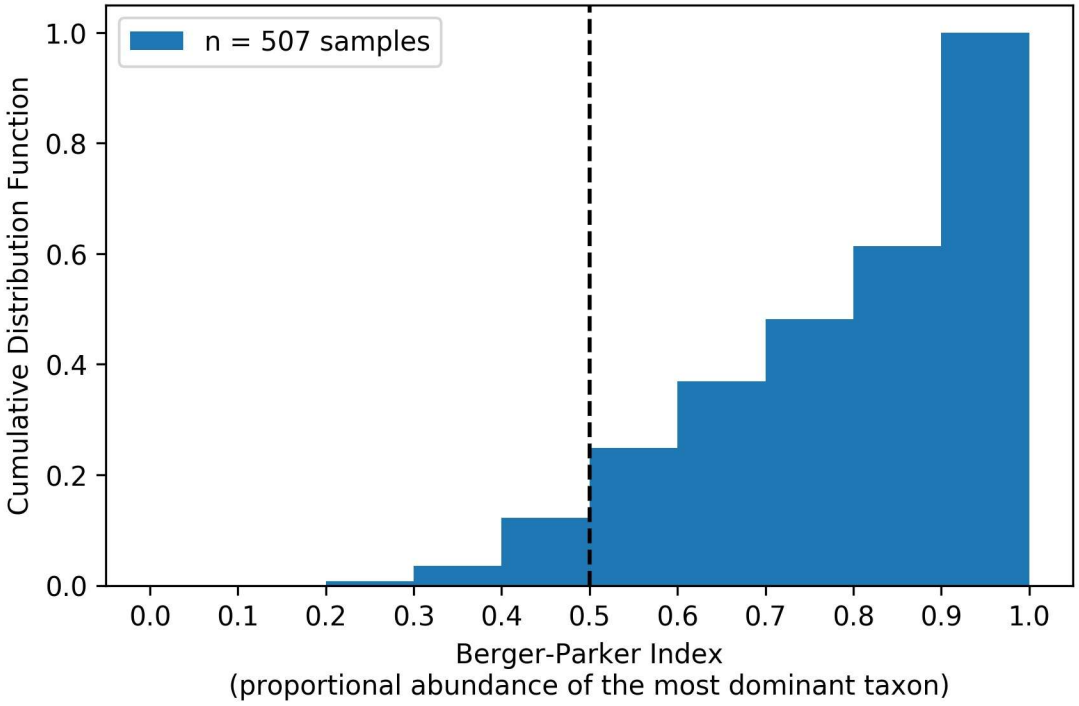

Figure S1: Cumulative distribution function of the Berger-Parker Index in the combined datasets.

479 # Supplementary Tables

480 *Table S1A: Predominant taxa of microbiotype 1.*

genus	Mean Relative Abundance (%)	Prevalence (%)
Corynebacterium	75.29	100
Staphylococcus	10.69	76.58
Alloiococcus	2.79	28.83
Moraxella	2.31	9.91
unidentified (Enterobacteriaceae)	1.41	15.32
unidentified (Neisseriaceae)	1.18	20.72
Streptococcus	1	21.62
Haemophilus	0.56	9.91
unidentified (Moraxellaceae)	0.44	2.7
Ralstonia	0.34	10.36

481

482 *Table S1B: Predominant taxa of microbiotype 2.*

genus	Mean Relative Abundance (%)	Prevalence (%)
Staphylococcus	74.96	100
Corynebacterium	9.87	64.1
Streptococcus	3.22	25.64
unidentified (Enterobacteriaceae)	1.82	15.38
Haemophilus	1.41	10.26
Moraxella	1.27	5.13
Ralstonia	1.19	11.97
Pseudomonas	1.05	6.84
Parvimonas	0.72	0.85
unidentified (Neisseriaceae)	0.61	7.69

483

484 *Table S1C: Predominant taxa of microbiotype 3.*

genus	Mean Relative Abundance (%)	Prevalence (%)
Haemophilus	23.78	40.85
Streptococcus	23.22	46.48
Moraxella	12.11	19.72
Pseudomonas	9.17	15.49
unidentified (Enterobacteriaceae)	5.74	9.86
Serratia	5.7	8.45
Klebsiella	2.75	4.23
Corynebacterium	2.56	46.48
Prevotella	1.44	12.68
Acinetobacter	1.38	1.41

485

486 *Table S2: Addressing previous criticism to gut enterotyping.*

Critique	Answer
Discrete clusters or a multi-dimensional gradient?	We acknowledge the a proportion of samples fall in the gradient between the proposed microbiotypes. Berger-Parker index investigation showed that most samples had one dominating taxon.
Do discrete clusters link to human disease?	No. We report that we could not find an association between the microbiotype and chronic sinusitis disease status.
Is sampling frame or selection bias affecting results?	No; Multi-centre international study with consecutive sampling methodology. We also validate on a separate dataset.
Use inappropriate visualization such as “star-burst plots”?	We did not use inappropriate visualizations.
Use a supervized approach “between-class analysis”?	We use an unsupervised clustering and dimensionality reduction approach.
Is an individual’s microbiotype stable over time?	Answer unknown; Future longitudinal studies required.

487

REFERENCES

1. Fokkens, W. J. *et al.* EPOS 2012: European position paper on rhinosinusitis and nasal polyps 2012. A summary for otorhinolaryngologists. *Rhinology* **50,** 1–12 (2012).

2. Paramasivan, S. *et al.* The international sinonasal microbiome study (ISMS): A multi centre, international characterization of sinonasal bacterial ecology. *bioRxiv* 548743 (2019). doi:10.1101/548743

3. Wagner Mackenzie, B. *et al.* Bacterial community collapse: A meta-analysis of the sinonasal microbiota in chronic rhinosinusitis. *Environmental Microbiology* **19,** 381–392 (2017).

4. Arumugam, M. *et al.* Enterotypes of the human gut microbiome. *Nature* **473,** 174–180 (2011).

5. Cope, E. K., Goldberg, A. N., Pletcher, S. D. & Lynch, S. V. Compositionally and functionally distinct sinus microbiota in chronic rhinosinusitis patients have immunological and clinically divergent consequences. *Microbiome* **5,** 53 (2017).

6. Legendre, P. & Legendre, L. *Numerical ecology*. (Elsevier, 2012).

7. McInnes, L., Healy, J. & Astels, S. Hdbscan: Hierarchical density based clustering. *The Journal of Open Source Software* **2,** 205 (2017).

8. Bolyen, E. *et al. QIIME 2: Reproducible, interactive, scalable, and extensible microbiome data science*. (PeerJ Inc., 2018). doi:10.7287/peerj.preprints.27295v1

9. Amir, A. *et al.* Deblur Rapidly Resolves Single-Nucleotide Community Sequence Patterns. *mSystems* **2,**

10. Thompson, L. R. *et al.* A communal catalogue reveals Earth's multiscale microbial diversity. *Nature* **551,** 457–463 (2017).

11. Barrow, G. I. Microbial Antagonism by Staphylococcus aureus. *Microbiology* **31,** 471–481 (1963).

12. Cleland, E. J. *et al.* Probiotic manipulation of the chronic rhinosinusitis microbiome. *International Forum of Allergy & Rhinology* **4,** 309–314 (2014).

13. Lina, G. *et al.* Bacterial competition for human nasal cavity colonization: Role of Staphylococcal agr alleles. *Applied and Environmental Microbiology* **69,** 18–23 (2003).

14. Jervis-Bardy, J., Foreman, A., Boase, S., Valentine, R. & Wormald, P.-J. What is the origin of Staphylococcus aureus in the early postoperative sinonasal cavity? *International Forum of Allergy & Rhinology* **1,** 308–312

15. Drilling, A. *et al.* Cousins, siblings, or copies: The genomics of recurrent Staphylococcus aureus infections in chronic rhinosinusitis. *International Forum of Allergy & Rhinology* **4,** 953–960 (2014).

16. Psaltis, A. J., Weitzel, E. K., Ha, K. R. & Wormald, P.-J. The effect of bacterial biofilms on post-sinus surgical outcomes. *American Journal of Rhinology* **22,** 1–6

17. Foreman, A. & Wormald, P.-J. Different biofilms, different disease? A clinical outcomes study. *The Laryngoscope* **120,** 1701–1706 (2010).

522 18. Singhal, D., Foreman, A., Bardy, J.-J. & Wormald, P.-J. Staphylococcus aureus biofilms: Nemesis of
523 endoscopic sinus surgery. *The Laryngoscope* **121,** 1578–1583 (2011).

524 19. Bachert, C., Zhang, N., Patou, J., van Zele, T. & Gevaert, P. Role of staphylococcal superantigens in
525 upper airway disease. *Current Opinion in Allergy and Clinical Immunology* **8,** 34–38 (2008).

526 20. Bendouah, Z., Barbeau, J., Hamad, W. A. & Desrosiers, M. Biofilm formation by Staphylococcus
527 aureus and Pseudomonas aeruginosa is associated with an unfavorable evolution after surgery for chronic
528 sinusitis and nasal polyposis. *Otolaryngology–Head and Neck Surgery: Official Journal of American*
529 *Academy of Otolaryngology-Head and Neck Surgery* **134,** 991–996 (2006).

530 21. Friedman, J. & Alm, E. J. Inferring Correlation Networks from Genomic Survey Data. *PLOS*
531 *Computational Biology* **8,** e1002687 (2012).

532 22. Bokulich, N. A. *et al.* Optimizing taxonomic classification of marker-gene amplicon sequences with
533 QIIME 2's q2-feature-classifier plugin. *Microbiome* **6,** 90 (2018).

534 23. Kaehler, B. D., Bokulich, N., Caporaso, J. G. & Huttley, G. A. Species-level microbial sequence
535 classification is improved by source-environment information. *bioRxiv* 406611 (2018).
536 doi:10.1101/406611

537 24. Wu, G. D. *et al.* Linking long-term dietary patterns with gut microbial enterotypes. *Science (New*
538 *York, N.Y.)* **334,** 105–108 (2011).

539 25. Vandeputte, D. *et al.* Stool consistency is strongly associated with gut microbiota richness and
540 composition, enterotypes and bacterial growth rates. *Gut* **65,** 57–62 (2016).

541 26. Jeffery, I. B., Claesson, M. J., O'Toole, P. W. & Shanahan, F. Categorization of the gut microbiota:
542 Enterotypes or gradients? *Nature Reviews. Microbiology* **10,** 591–592 (2012).

543 27. Koren, O. *et al.* A Guide to Enterotypes across the Human Body: Meta-Analysis of Microbial
544 Community Structures in Human Microbiome Datasets. *PLOS Computational Biology* **9,** e1002863
545 (2013).

546 28. Knights, D. *et al.* Rethinking 'Enterotypes'. *Cell host & microbe* **16,** 433–437 (2014).

547 29. Costea, P. I. *et al.* Enterotypes in the landscape of gut microbial community composition. *Nature*
548 *Microbiology* **3,** 8–16 (2018).

549 30. Berger, W. H. & Parker, F. L. Diversity of planktonic foraminifera in deep-sea sediments. *Science*
550 *(New York, N.Y.)* **168,** 1345–1347 (1970).

551 31. Gonzalez, A. *et al.* Qiita: Rapid, web-enabled microbiome meta-analysis. *Nature Methods* **15,** 796–
552 798 (2018).

553 32. Zhang, J., Kobert, K., Flouri, T. & Stamatakis, A. PEAR: A fast and accurate Illumina Paired-End
554 reAd mergeR. *Bioinformatics* **30,** 614–620 (2014).

555 33. Bokulich, N. A. *et al.* Quality-filtering vastly improves diversity estimates from Illumina amplicon
556 sequencing. *Nature Methods* **10,** 57–59 (2013).

557 34. Wang, J. *et al. Minimizing spurious features in 16S rRNA gene amplicon sequencing*. (PeerJ Inc.,
558 2018). doi:10.7287/peerj.preprints.26872v1

559 35. Janssen, S. *et al.* Phylogenetic Placement of Exact Amplicon Sequences Improves Associations with
560 Clinical Information. *mSystems* **3,**

561 36. DeSantis, T. Z. *et al.* Greengenes, a Chimera-Checked 16S rRNA Gene Database and Workbench
562 Compatible with ARB. *Applied and Environmental Microbiology* **72,** 5069–5072 (2006).

563 37. Pedregosa, F. *et al.* Scikit-learn: Machine Learning in Python. *Journal of Machine Learning Research*
564 **12,** 2825–2830 (2011).

565 38. Mandal, S. *et al.* Analysis of composition of microbiomes: A novel method for studying microbial
566 composition. *Microbial Ecology in Health and Disease* **26,** 27663 (2015).

567 39. Watts, S. C., Ritchie, S. C., Inouye, M. & Holt, K. E. FastSpar: Rapid and scalable correlation
568 estimation for compositional data. *bioRxiv* 272583 (2018). doi:10.1101/272583

569 40. Chan, C. L. *et al.* The microbiome of otitis media with effusion. *The Laryngoscope* **126,** 2844–2851
570 (2016).

571 41. Yu, Y., Lee, C., Kim, J. & Hwang, S. Group-specific primer and probe sets to detect methanogenic
572 communities using quantitative real-time polymerase chain reaction. *Biotechnology and Bioengineering*
573 **89,** 670–679 (2005).

574 42. Kluyver, T. *et al.* Jupyter Notebooks a publishing format for reproducible computational workflows.
575 in *Positioning and Power in Academic Publishing: Players, Agents and Agendas* (eds. Loizides, F. &
576 Scmidt, B.) 87–90 (IOS Press, 2016). doi:10.3233/978-1-61499-649-1-87

577 43. Oliphant, T. E. Python for Scientific Computing. *Computing in Science & Engineering* **9,** 10–20
578 (2007).